Supporting Information

Non-precious catalyst for three-phase contact in Proton Exchange Membrane CO_2 conversion full cell for efficient electrochemical reduction of carbon dioxide

Sreetama Ghosh, Meenakshi Seshadhri Garapati†, Arpita Ghosh† and Ramaprabhu Sundara*

*Alternative Energy and Nanotechnology Laboratory (AENL), Nano Functional Materials Technology Center (NFMTC), Department of Physics, Indian Institute of Technology Madras, Chennai 600036, India; *Phone: +91-44-22574862; fax: +91-44-22570509.*

**E-mail: ramp@iitm.ac.in*

† These authors have equal contribution

Table S1 Standard electrochemical reduction potentials.

Reactions	**E^0 (V) vs NHE at pH 7**
$CO_2 + e^- \rightarrow CO_2^{\cdot -}$	–1.90
$CO_2 + 2H^+ + 2e^- \rightarrow HCOOH$	–0.61
$CO_2 + 2H^+ + 2e^- \rightarrow CO + H_2O$	–0.52
$CO_2 + 4H^+ + 4e^- \rightarrow HCHO + H_2O$	–0.48
$CO_2 + 6H^+ + 6e^- \rightarrow CH_3OH + H_2O$	–0.38
$CO_2 + 8H^+ + 8e^- \rightarrow CH_4 + 2H_2O$	–0.24
$2H^+ + 2e^- \rightarrow H_2$	–0.41

Table S2 Comparison of the present work with reported literature.

Materials	Cell	Main product	F.E. (%)	Stability (h)	Ref.
NCNTs	Flow cell	CO	80	10	[1]
N-graphene	H-cell	HCOOH	66	4	[2]
PEI-NCNTs	H-cell	HCOOH	87	24	[3]
Au/NC	H-cell	CO	~ 83	2	[4]
Fe-N-C	H-cell	CO	85	-	[5]
Fe-N-C	H-cell	CO	91	6	[6]
Ni-N-C	H-cell	CO	71.9	60	[7]
Sn-N-C	H-cell	HCOOH	74.3	200	[8]
Fe-N_4-graphene	H-cell	CO	~ 80	10	[9]
Fe_3C@NCNTs	**PEM CO_2 conversion cell**	**HCOOH**	**~ 90**	**24**	**Present work**

Table S3 Elemental compositions of Fe_3C@NCNTs and NCNTs has been determined by XPS.

Samples	Elemental composition (at %)			
	C 1s	N 1s	Fe 2p	O 1s
Fe_3C@NCNTs	91.6	4.2	1.8	2.4
NCNTs	93.2	4.8	-	2

An appreciably high N-doping of 4.8 at % was obtained for NCNTs and around 4.2 at % was obtained for Fe_3C@NCNTs. XPS revealed low surface metal contents in all the samples in comparison to that obtained by ICP-OES implying that XPS measurement was only sensitive to surface elements and in most of the cases the metal nanoparticles were encapsulated by carbon layers.

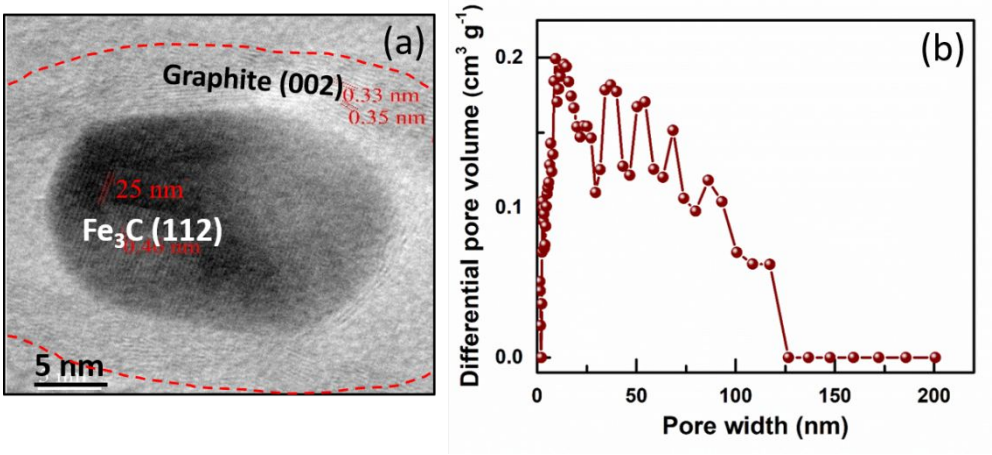

Figure S1. (a) HRTEM image of Fe_3C@NCNTs (red dashed lines, shown on either side, distinguish between the graphitic coating on the encapsulated nanoparticle and the amorphous carbon substrate) and (b) NLDFT pore-size distribution curve of Fe_3C@NCNTs.

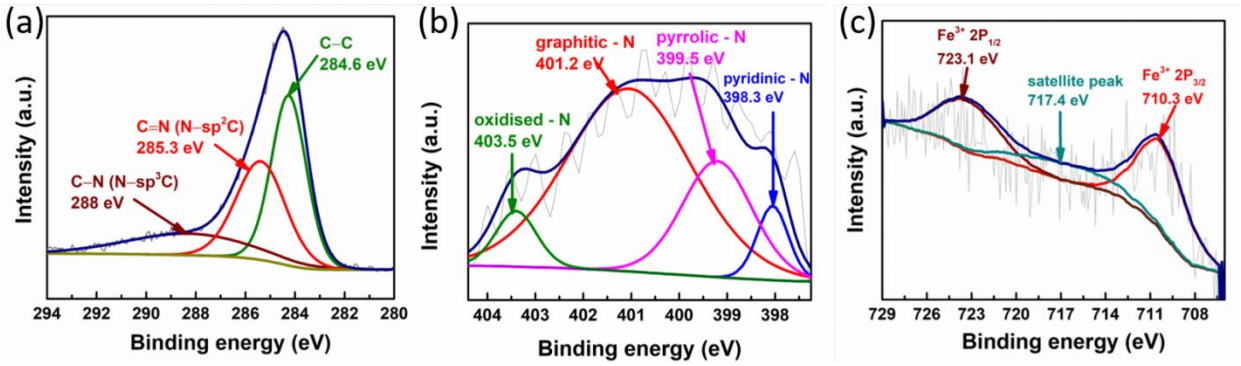

Figure S2. High resolution XPS spectra of (a) C 1s, (b) N 1s, (c) Fe 2p respectively of Fe_3C@NCNTs.

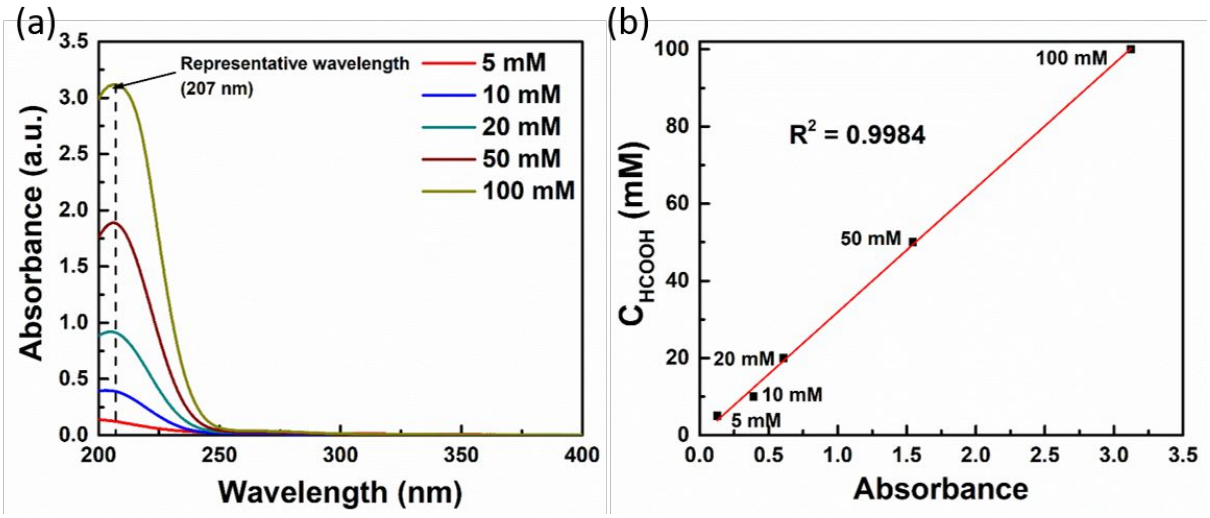

Figure S3. Quantification of formic acid formed from CO_2 reduction by UV spectroscopy, (a) UV-Vis absorption spectra for different concentrations of commercial formic acid and (b) Calibration curve for the measurement of formic acid generated by CO_2 electroreduction.

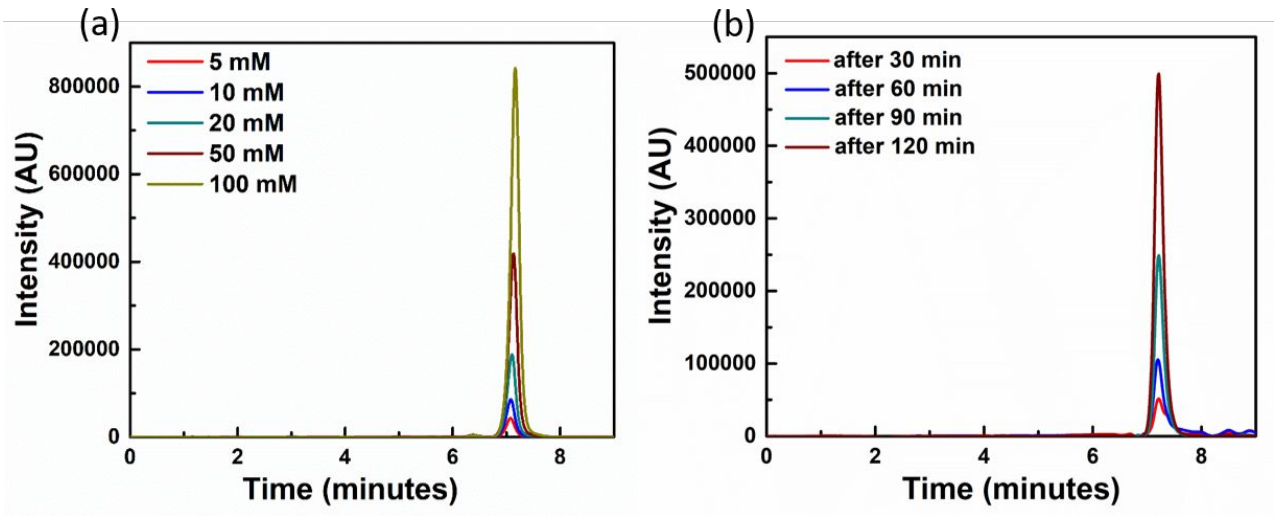

Figure S4. (a) Chromatograms with standard formic acid solutions and (b) HPLC product analysis results of liquid phase samples generated from electrochemical CO_2 reduction with Fe_3C@NCNTs on both anode as well as cathode. HCOOH peak appears in both at a retention time of 7.2 min.

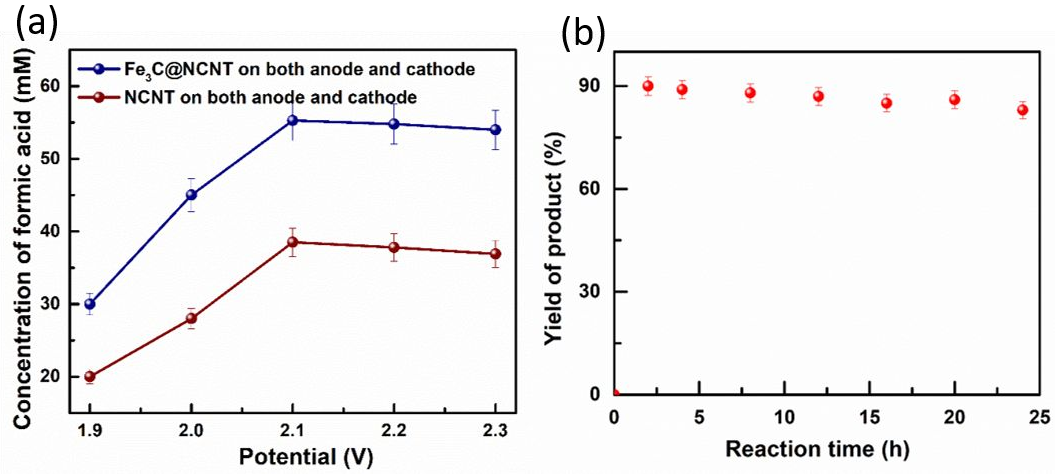

Figure S5. (a) Determination of working potential for PEM CO_2 conversion cell after 120 min conversion time for each data and (b) durability test of full cell system for continuous formic acid formation with Fe_3C@NCNTs on both anode as well as cathode.

References:

(1) Wu, J.; Yadav, R. M.; Liu, M.; Sharma, P. P.; Tiwary, C. S.; Ma, L.; Zou, X.; Zhou, X.-D.; Yakobson, B. I.; Lou, J.; Ajayan, P. M.; Achieving Highly Efficient, Selective, and Stable CO_2 Reduction on Nitrogen-Doped Carbon Nanotubes. *ACS Nano* **2015**, *9* (5), 5364–5371.

(2) Wang, H.; Chen, Y.; Hou, X.; Ma, C.; Tan, T. Nitrogen-Doped Graphenes as Efficient Electrocatalysts for the Selective Reduction of Carbon Dioxide to Formate in Aqueous Solution. *Green Chem.* **2016**, *18* (11), 3250–3256.

(3) Zhang, S.; Kang, P.; Ubnoske, S.; Brennaman, M. K.; Song, N.; House, R. L.; Glass, J. T.; Meyer, T. J. Polyethylenimine-Enhanced Electrocatalytic Reduction of CO_2 to Formate at Nitrogen-Doped Carbon Nanomaterials. *J. Am. Chem. Soc.* **2014**, *136* (22), 7845–7848.

(4) Jin, L.; Liu, B.; Wang, P.; Yao, H.; Achola, L. A.; Kerns, P.; Lopes, A.; Yang, Y.; Ho, J.; Moewes, A.; Pei, Y.; He, J.; Ultrasmall Au Nanocatalysts Supported on Nitrided Carbon for Electrocatalytic CO_2 Reduction: The Role of the Carbon Support in High Selectivity. *Nanoscale* **2018**, *10* (30), 14678–14686.

(5) Leonard, N.; Ju, W.; Sinev, I.; Steinberg, J.; Luo, F.; Varela, A. S.; Roldan Cuenya, B.; Strasser, P. The Chemical Identity, State and Structure of Catalytically Active Centers during the Electrochemical CO_2 Reduction on Porous Fe-Nitrogen-Carbon (Fe-N-C) Materials. *Chem. Sci.* **2018**, *9* (22), 5064–5073.

(6) Huan, T. N.; Ranjbar, N.; Rousse, G.; Sougrati, M.; Zitolo, A.; Mougel, V.; Jaouen, F.; Fontecave, M. Electrochemical Reduction of CO_2 Catalyzed by Fe-N-C Materials: A Structure–Selectivity Study. *ACS Catal.* **2017**, *7* (3), 1520–1525.

(7) Zhao, C.; Dai, X.; Yao, T.; Chen, W.; Wang, X.; Wang, J.; Yang, J.; Wei, S.; Wu, Y.; Li, Y. Ionic Exchange of Metal-Organic Frameworks to Access Single Nickel Sites for Efficient Electroreduction of CO_2. *J. Am. Chem. Soc.* **2017**, *139* (24), 8078–8081.

(8) Zu, X.; Li, X.; Liu, W.; Sun, Y.; Xu, J.; Yao, T.; Yan, W.; Gao, S.; Wang, C.; Wei, S.; Xie, Y.; Efficient and Robust Carbon Dioxide Electroreduction Enabled by Atomically

Dispersed $Sn^{\delta+}$ Sites. *Adv. Mater.* **2019**, *31* (15), 1–8.

(9) Gu, J.; Hsu, C. S.; Bai, L.; Chen, H. M.; Hu, X. Atomically Dispersed Fe^{3+} Sites Catalyze Efficient CO_2 Electroreduction to CO. *Science.* **2019**, *364* (6445), 1091–1094.